

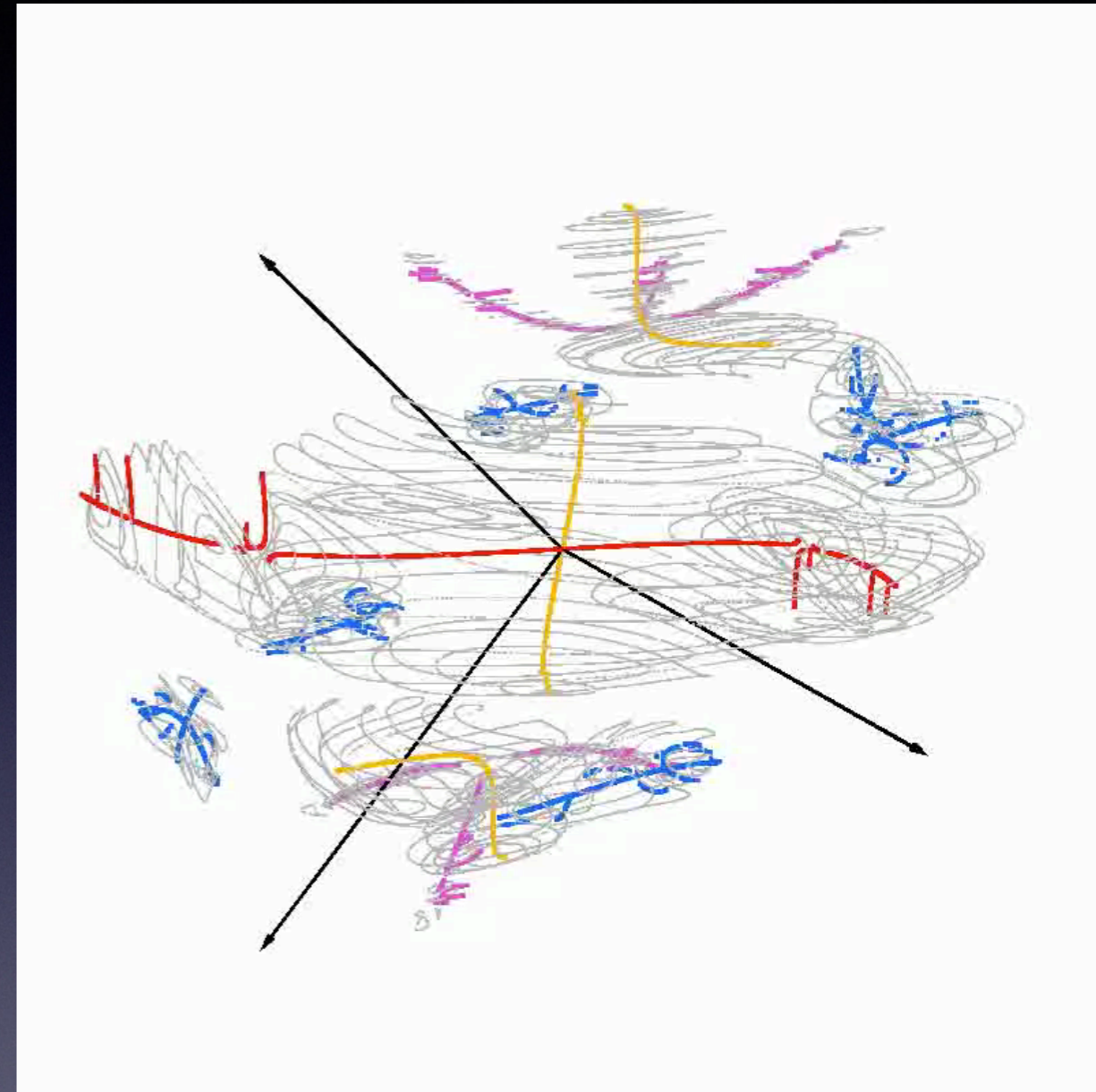
Visualizing Chaotic and Regular Orbits in Three and Four Dimensional Maps

James Meiss
University of Colorado at Boulder

Collaborators:
Arnd Bäcker, Holger Dullin,
Adam Fox, Nathan Guillery

Visualization: Geometry

- Phase Portraits (2D & 3D)
- Projections
 - Color for a missing dimension
- Slices
 - 4D \Rightarrow 2D: Kaneko-Bagley (1985), Kook-Meiss (1989)
 - 3D \Rightarrow 2D: Artuso-Casati- Shepelyansky (1992), Cartwright-Feingold-Piro (1994)
 - 4D \Rightarrow 3D: Richter-Lange-Bäcker-Ketzmerick (2014)
- Cube Plots
 - Assembled Slices: Lega-Guzzo-Froeschlé (2016)



Lange, S., M. Richter, et al. (2014). "Global structure of regular tori in a generic 4D symplectic map." Chaos 24: 024409.

Visualization: Indicators

- Chaos

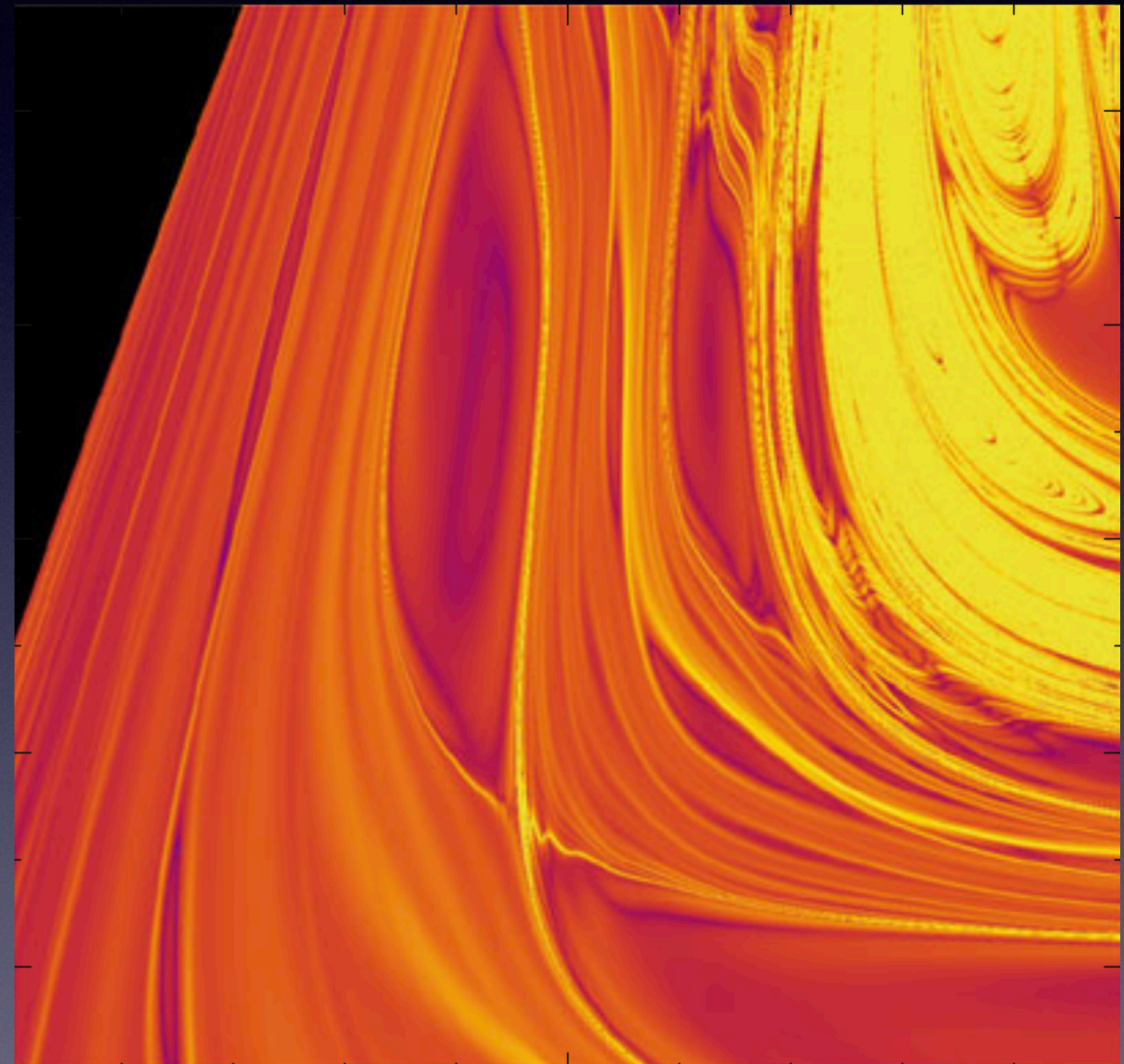
- Fast Lyapunov Indicator (FLI): Froeschlé-Gonczi-Lega (1997)
- Finite Time Lyapunov (FTLE): Haller (2000)
- Smaller Alignment Index (SALI): Skokos (2001)
- Lagrangian Coherent Structures (LCS): Shadden-Leiken -Marsden (2005)
- Lagrangian Descriptors: Madrid-Mancho (2009)

- Regularity

- Resonance Partitions: MacKay-Meiss-Percival (1987)
- Frequency Maps: Laskar (1992)
- Width (a Lagrangian Indicator): Easton-Meiss-Carver (1993)
- Ergodic Partition: Mezić-Wiggins (2001)
- Parameterization Method (tori): Cabré-Fontich-de la Llave (2003)

- Transport

- Drift/Diffusion: Chirikov (1979)
- Exit Time Distributions: Karney (1982)
- Action Diameter: Meiss-Guillery (2017)



Lega, E., M. Guzzo and C. Froeschle (2016). Theory and Applications of the FLI Method. Chaos Detection and Predictability Springer. 915: 35-54.

Angle-Action Maps

- Standard (angle-action) form on $\mathbb{T}^n \times \mathbb{R}^m$

$$x' = x + \Omega(y') \pmod{1}$$

$$y' = y + F(x)$$

Angle-Action Form

insert "new" y here!

m actions

- Note: number of angles and actions can be different, $n \neq m$
- Frequency map

$$\Omega : \mathbb{R}^m \rightarrow \mathbb{T}^n$$

- Force

$$F : \mathbb{T}^n \rightarrow \mathbb{R}^m$$

Angle-Action Maps

- Symplectic Examples: ($n = m$)

- Chirikov's Standard map (1,1) $(x', y') = (x + y', y - \varepsilon \sin(2\pi x))$

- Froeschlé map (2,2) $(x', y') = (x + y', y - \varepsilon \nabla V(x))$

- Volume-Preserving Normal form (2,1)

$$\Omega = (\Omega_1(y), \Omega_2(y))$$

$$x'_1 = x_1 + y' + \gamma$$

$$x'_2 = x_2 + \beta y'^2 - \delta$$

$$y' = y - \varepsilon [\sin(2\pi x_1) + \sin(2\pi x_2) + \sin(2\pi(x_1 - x_2))]$$

3D Dynamics:
Invariant Tori
&
Frequency Maps

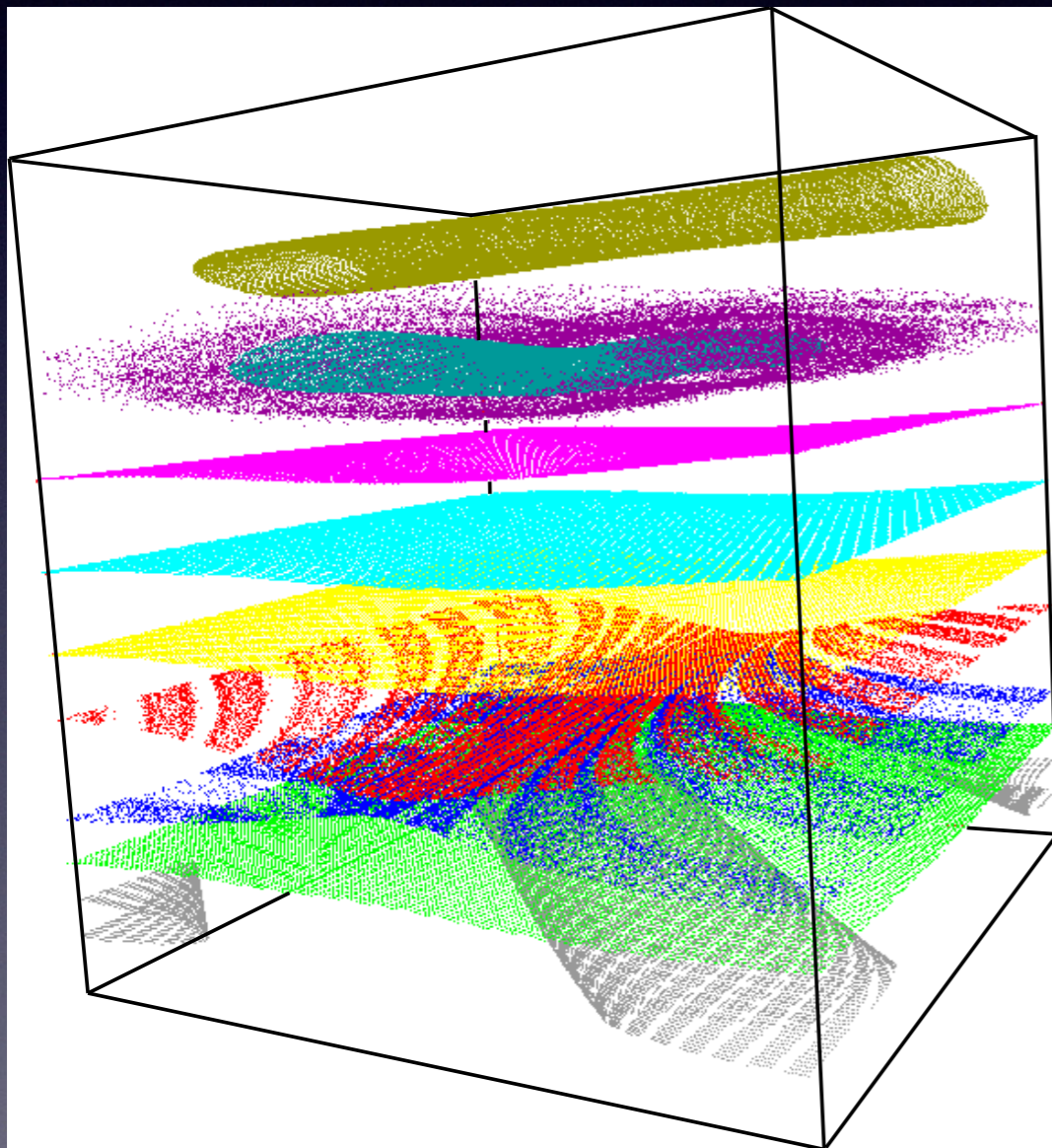
$$x'_1 = x_1 + y' + \gamma$$

$$x'_2 = x_2 + \beta y'^2 - \delta$$

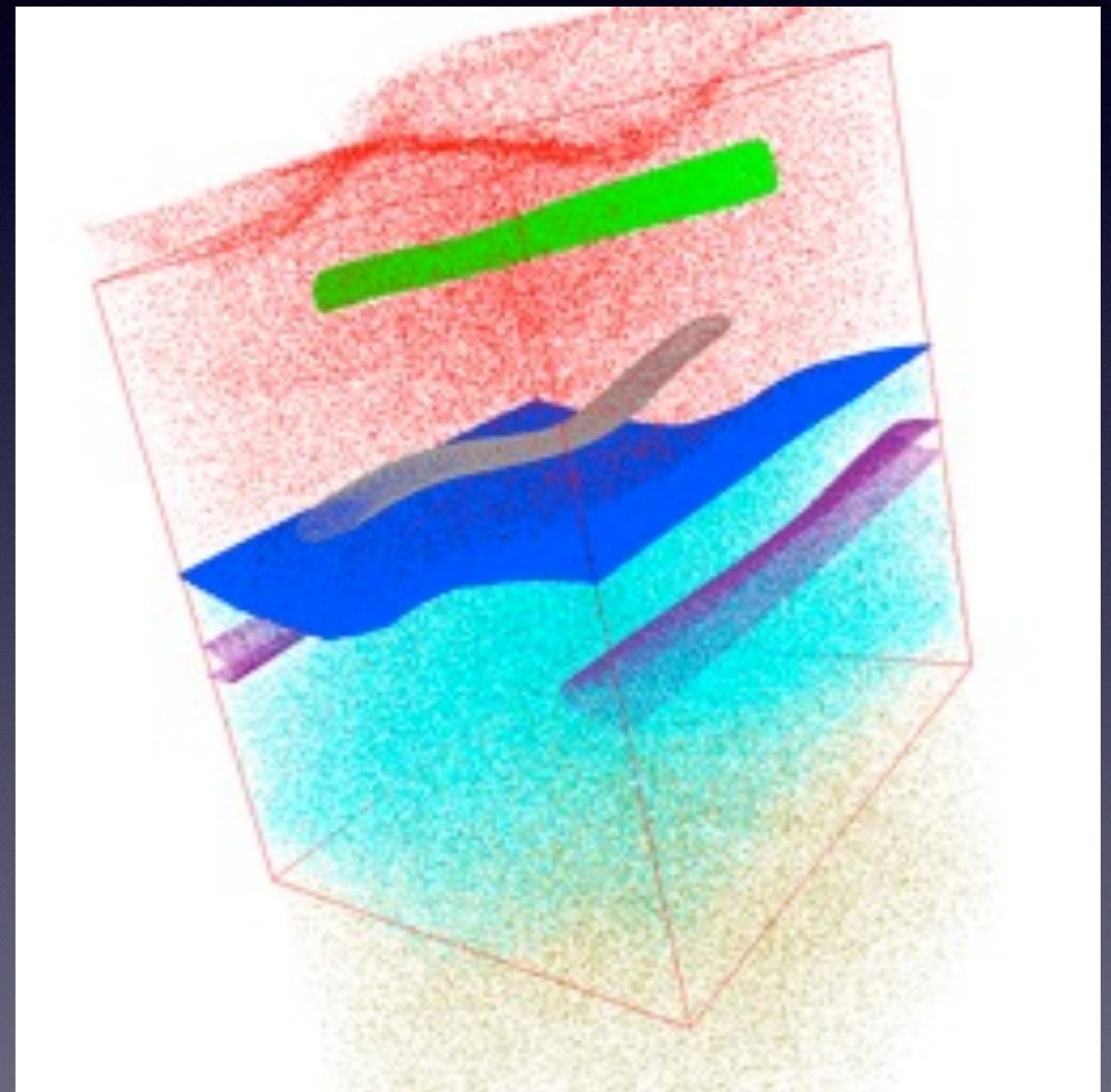
$$y' = y - \varepsilon[\sin(2\pi x_1) + \sin(2\pi x_2) + \sin(2\pi(x_1 - x_2))]$$

Many rotational tori

Only one rotational torus



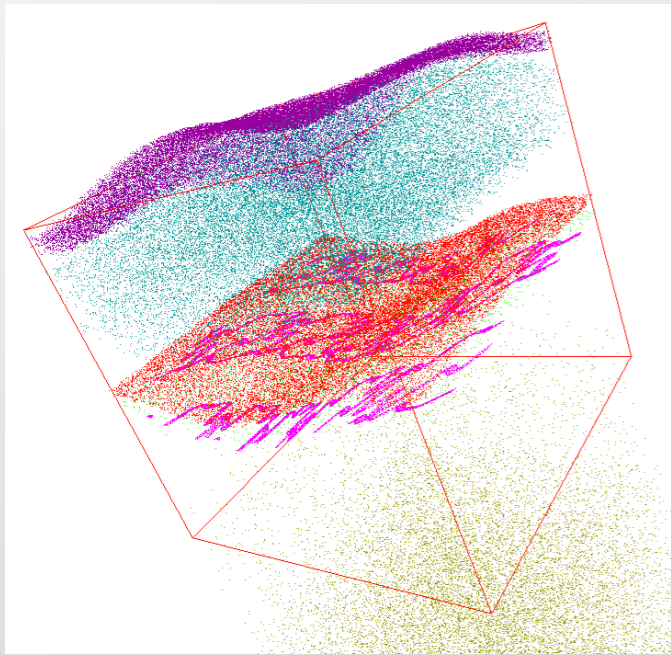
$\varepsilon = 0.005$



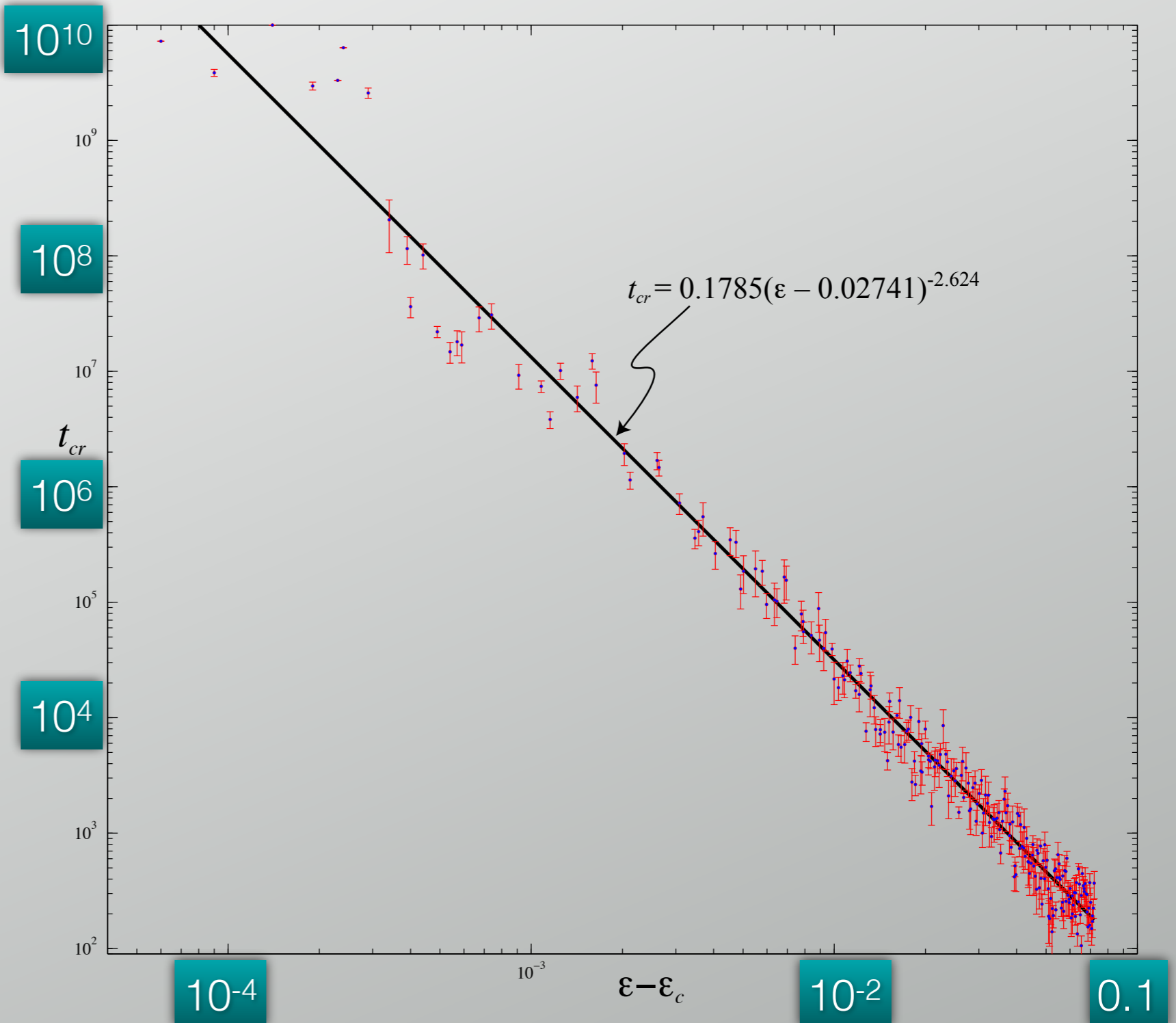
$\varepsilon = 0.02725$

$\beta = 2, \delta = 0.1, \gamma = \frac{1}{2}(1+\sqrt{5})$

Destruction \Rightarrow Transport



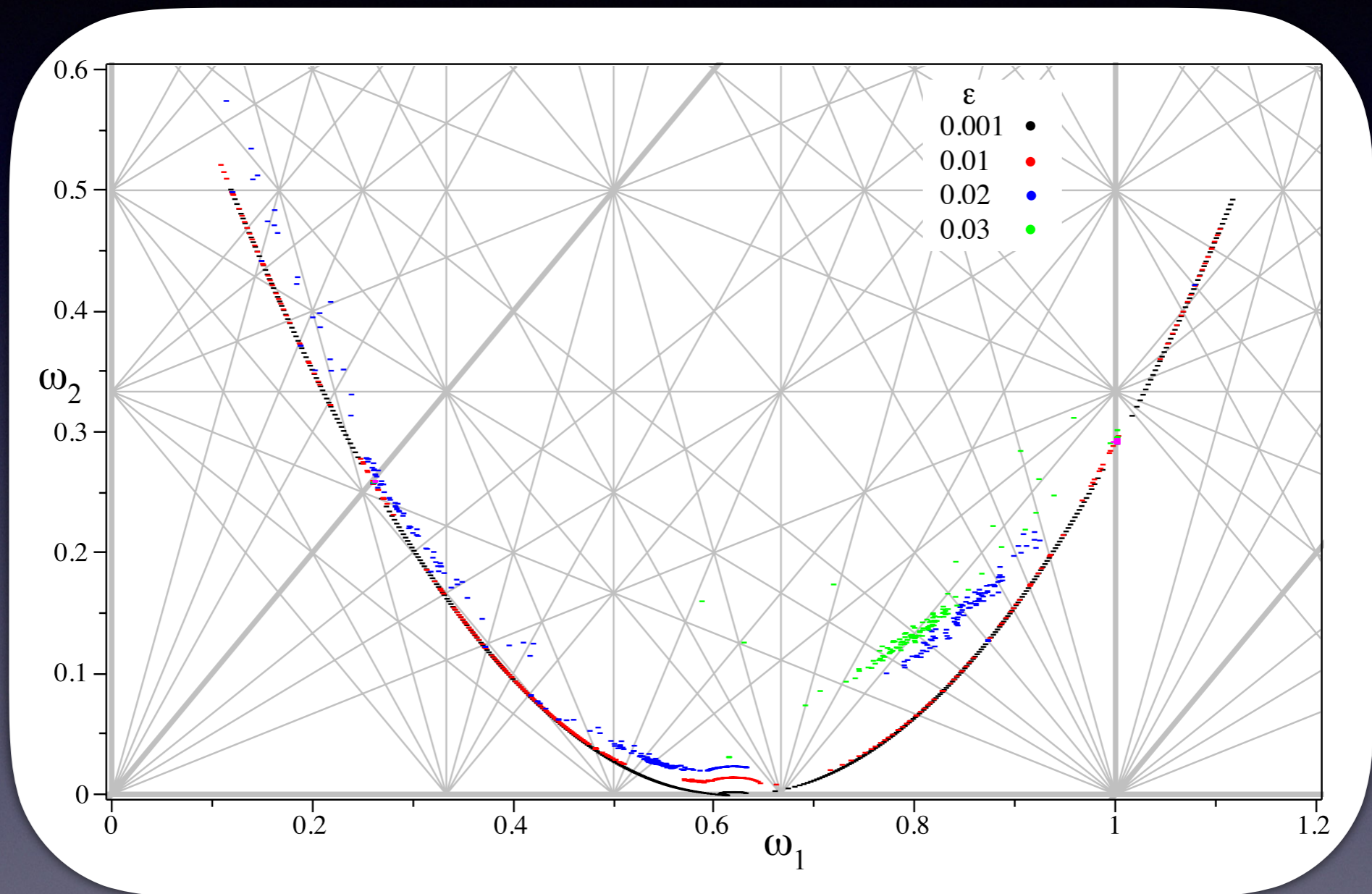
Crossing Time vs. $\epsilon - \epsilon_{cr}$
 $\delta = 0.1$
 $\epsilon_{cr} \approx 0.02741$



Meiss, J. D. (2012). "The Destruction of Tori in Volume-Preserving Maps." *Comm. Nonl. Sci and Num. Sim.* 17: 2108-2121.

Frequency Maps

- Varying Force Amplitude, ε .



$$x'_1 = x_1 + y' + \gamma$$

$$x'_2 = x_2 + \beta y'^2 - \delta$$

$$y' = y - \varepsilon [\sin(2\pi x_1) + \sin(2\pi x_2) + \sin(2\pi(x_1 - x_2))]]$$

$$\Omega : \mathbb{R} \rightarrow \mathbb{T}^2$$

$$\gamma = \frac{\sqrt{5}-1}{2}, \beta = 2, \delta = 0.1$$

4D Dynamics Projections & Slices

Fast Lyapunov Indicator

- Iterate arbitrarily chosen initial deviation v_0
- Compute the supremum up to time T

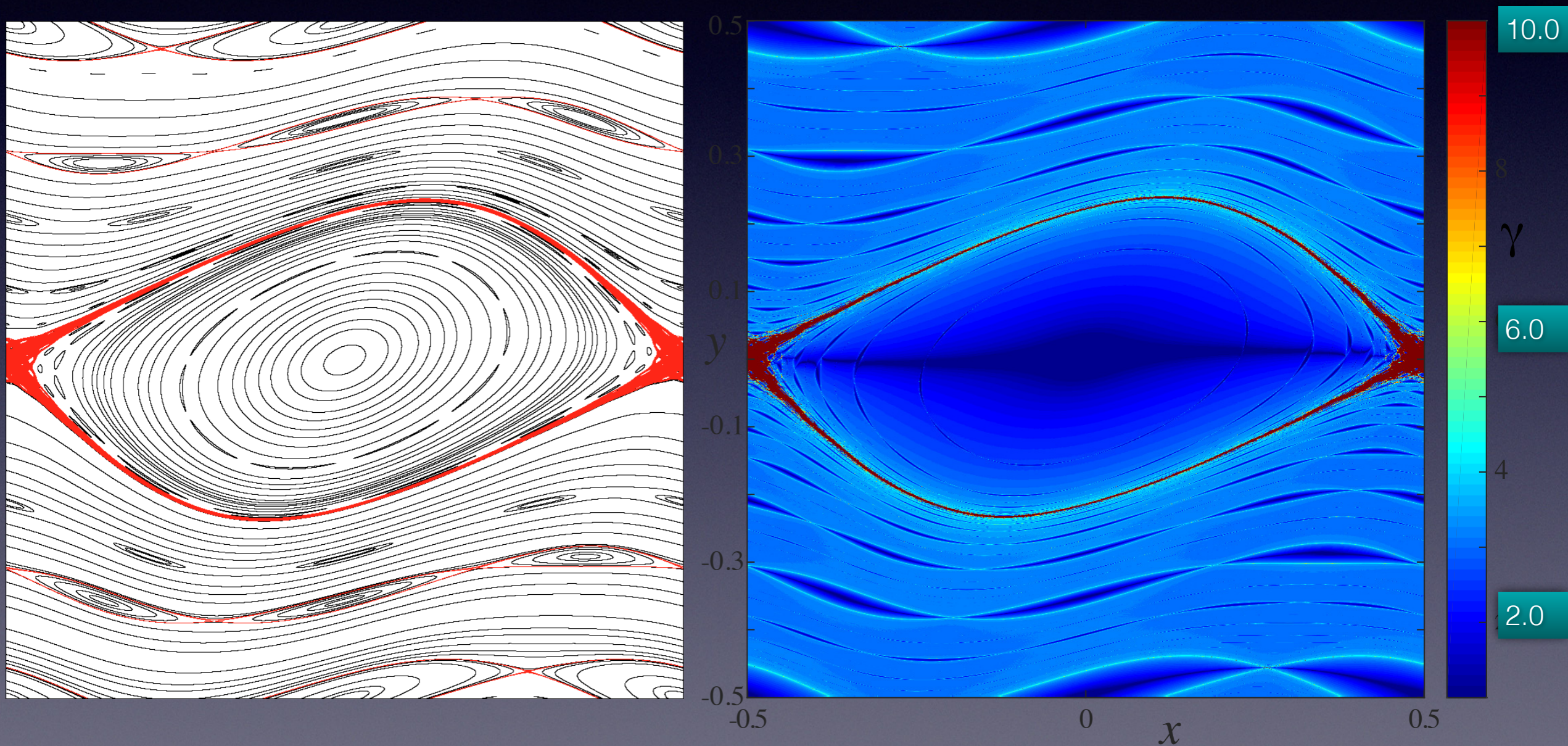
$$FLI = \sup_{t < T} (\log_{10} \|Df^t(z_0)v_0\|)$$

- similar to FTLE, but supremum reduces oscillations

Froeschle, C., R. Gonczi and E. Lega (1997). "The fast Lyapunov indicator: a simple tool to detect weak chaos. Planetary and Space Science 45(7): 881-886.

FLI: 2D Standard Map

$$FLI = \sup_{t < T} (\log_{10} \|Df^t(z_0)v_0\|)$$



- $a = 0.52$, $T = 10^3$, grid of 10^6 points

Froeschlé 4D Map

$$\begin{aligned}x' &= x + y' \pmod{1} \\ y' &= y + F(x)\end{aligned}$$

two angles

two actions

$$m = n = 2$$

- Froeschlé-like forces

$$F = -\frac{1}{2\pi} \begin{pmatrix} a \sin(2\pi x_1) & + & c \sin(2\pi(x_1 + x_2)) \\ b \sin(2\pi x_2) & + & c \sin(2\pi(x_1 + x_2 + \varphi)) \end{pmatrix}$$

- $\varphi = 0$: Symplectic since $F = -\nabla V$
- $\varphi = \frac{1}{2}$: “maximally non-symplectic” coupling

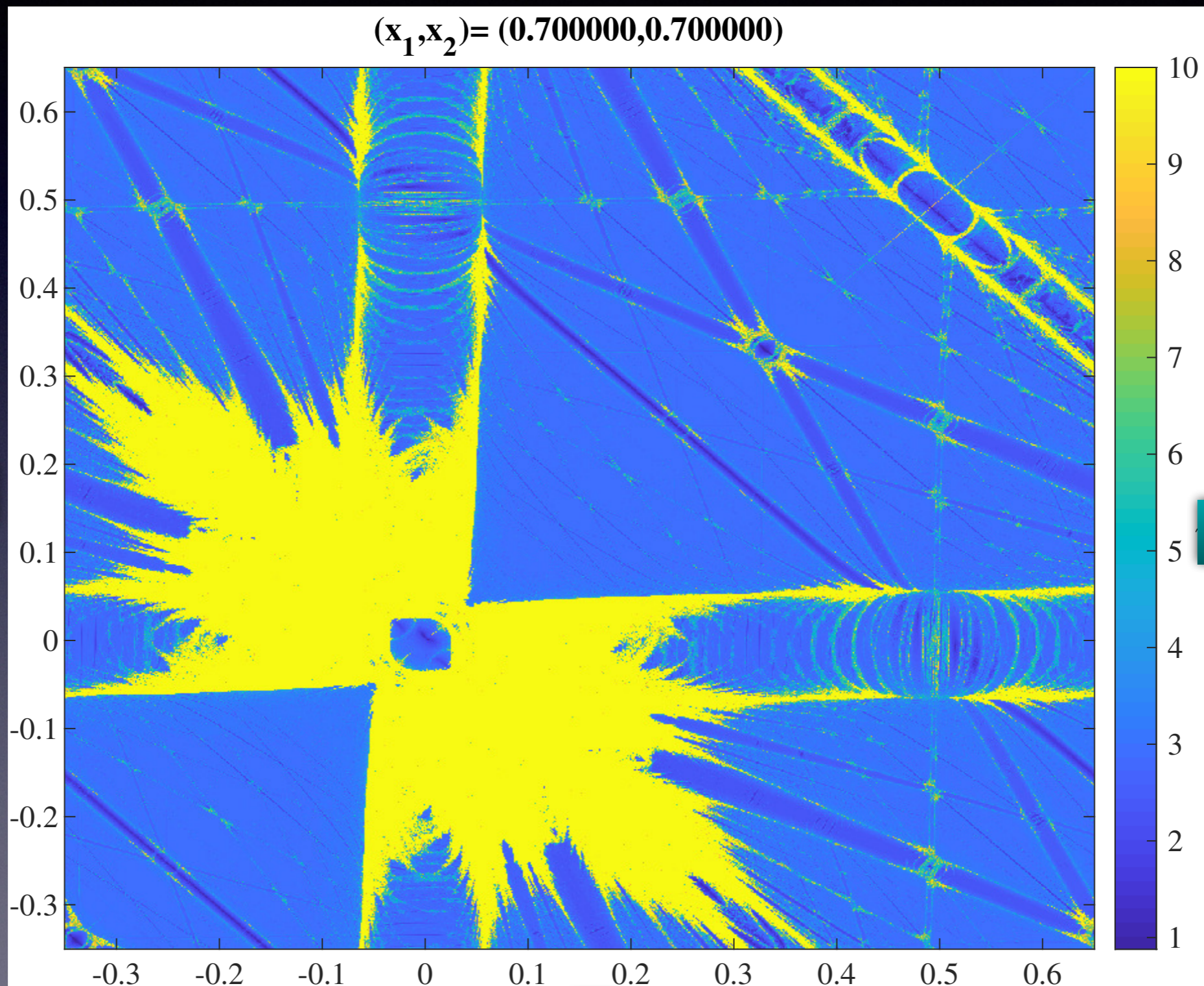
- Full Spectrum Force:

$$F_{fs} = -\frac{1}{2\pi} \frac{d}{(2.1 + \cos(2\pi x_1) + \cos(2\pi x_2))^2} \begin{pmatrix} \sin(2\pi x_1) \\ \sin(2\pi(x_2 + \varphi)) \end{pmatrix}$$

2D Slices: Action Plane

Varying ($x_1 = x_2$) Slices

$$FLI = \sup_{t < T} (\log_{10} \|Df^t(z_0)v_0\|)$$



y_2

$FLI, T = 1000$

$a = 0.1$
 $b = 0.1$
 $c = 0.07$
 $\varphi = 0$

y_1

Cube Plots: 3 Slices

$y_1 = 0.65$
 $x_1 = 0$

$y_2 = 0.65$
 $x_2 = 0$

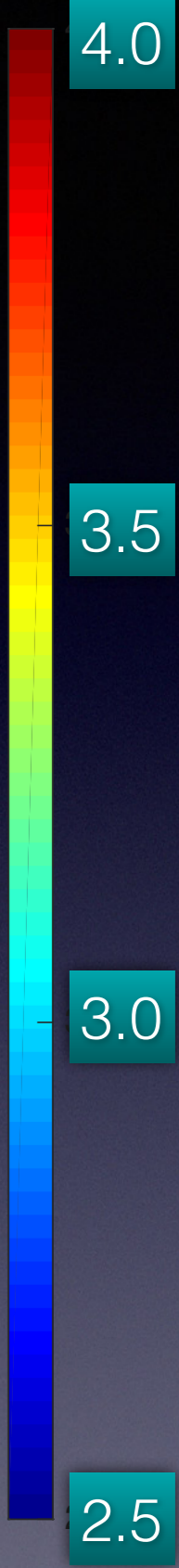
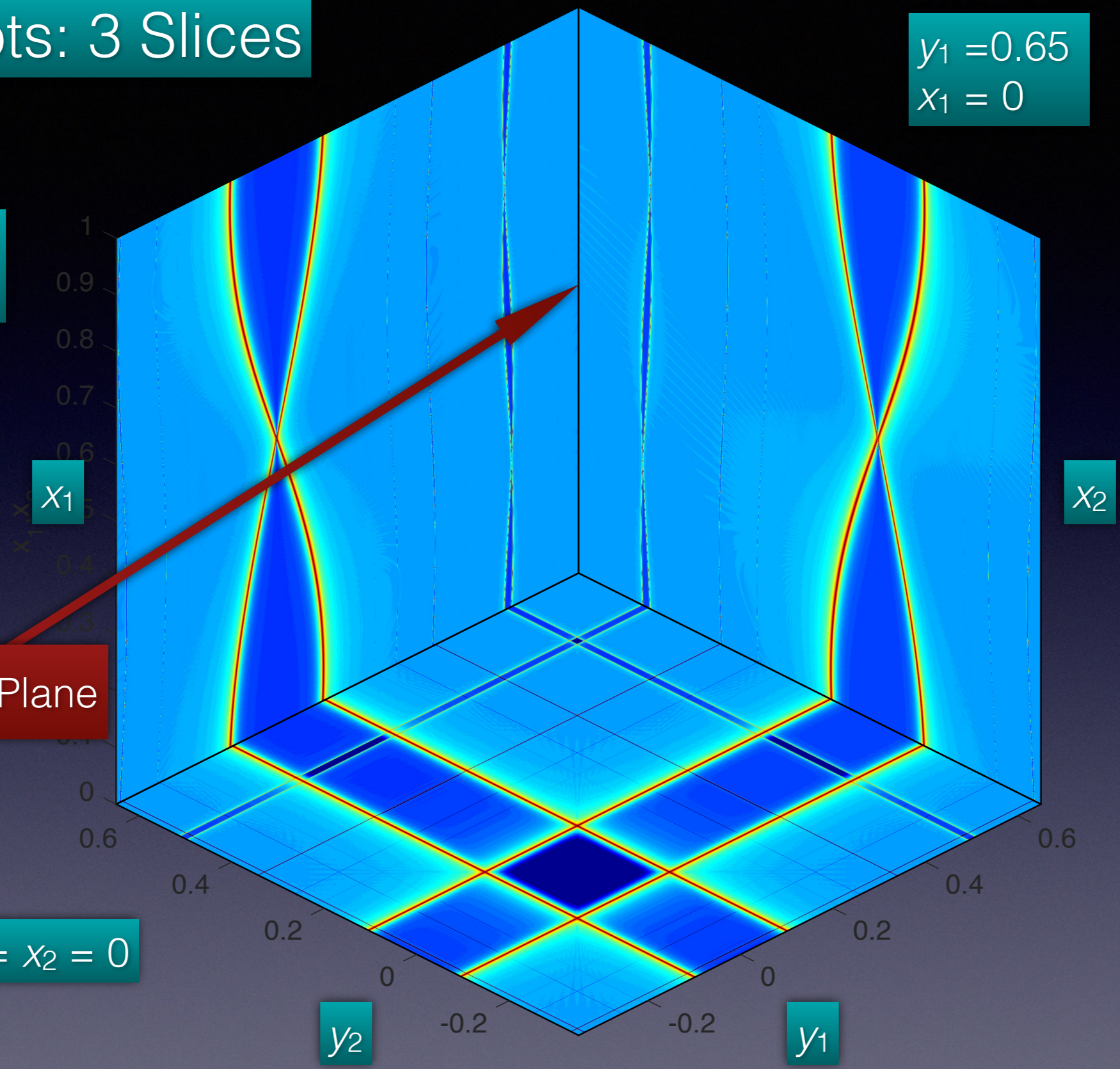
Two-Plane

$a = 0.1$
 $b = 0.1$
 $c = 0$
 $d = 0$
 $\varphi = 0$

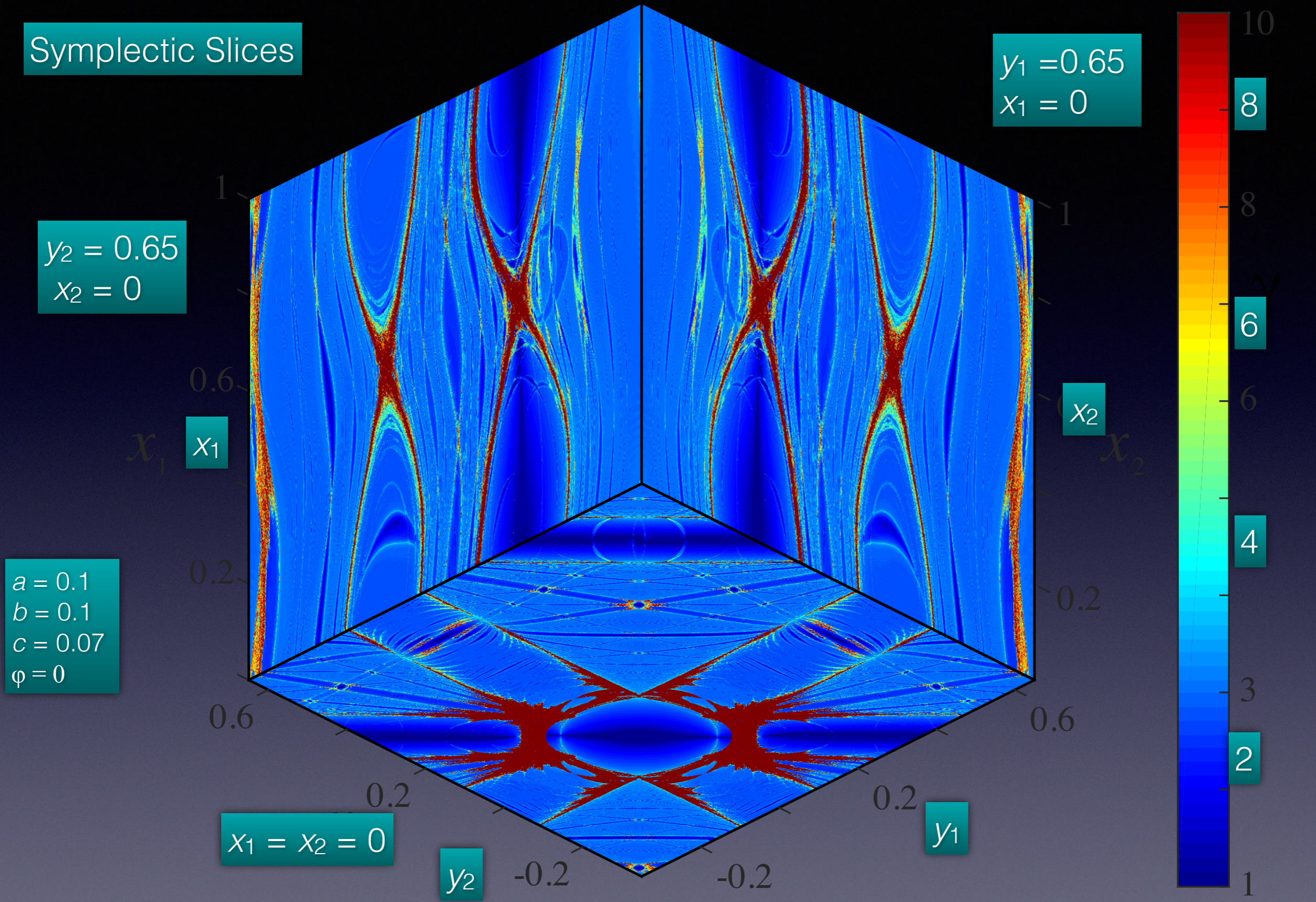
$x_1 = x_2 = 0$

FLI, $T = 1000$

$$F = -\frac{1}{2\pi} \begin{pmatrix} a \sin(2\pi x_1) \\ b \sin(2\pi x_2) \end{pmatrix}$$



Symplectic Slices



$a = 0.1$
 $b = 0.1$
 $c = 0.07$
 $\varphi = 0$

$y_1 = 0.65$
 $x_1 = 0$

$y_2 = 0.65$
 $x_2 = 0$

$x_1 = x_2 = 0$

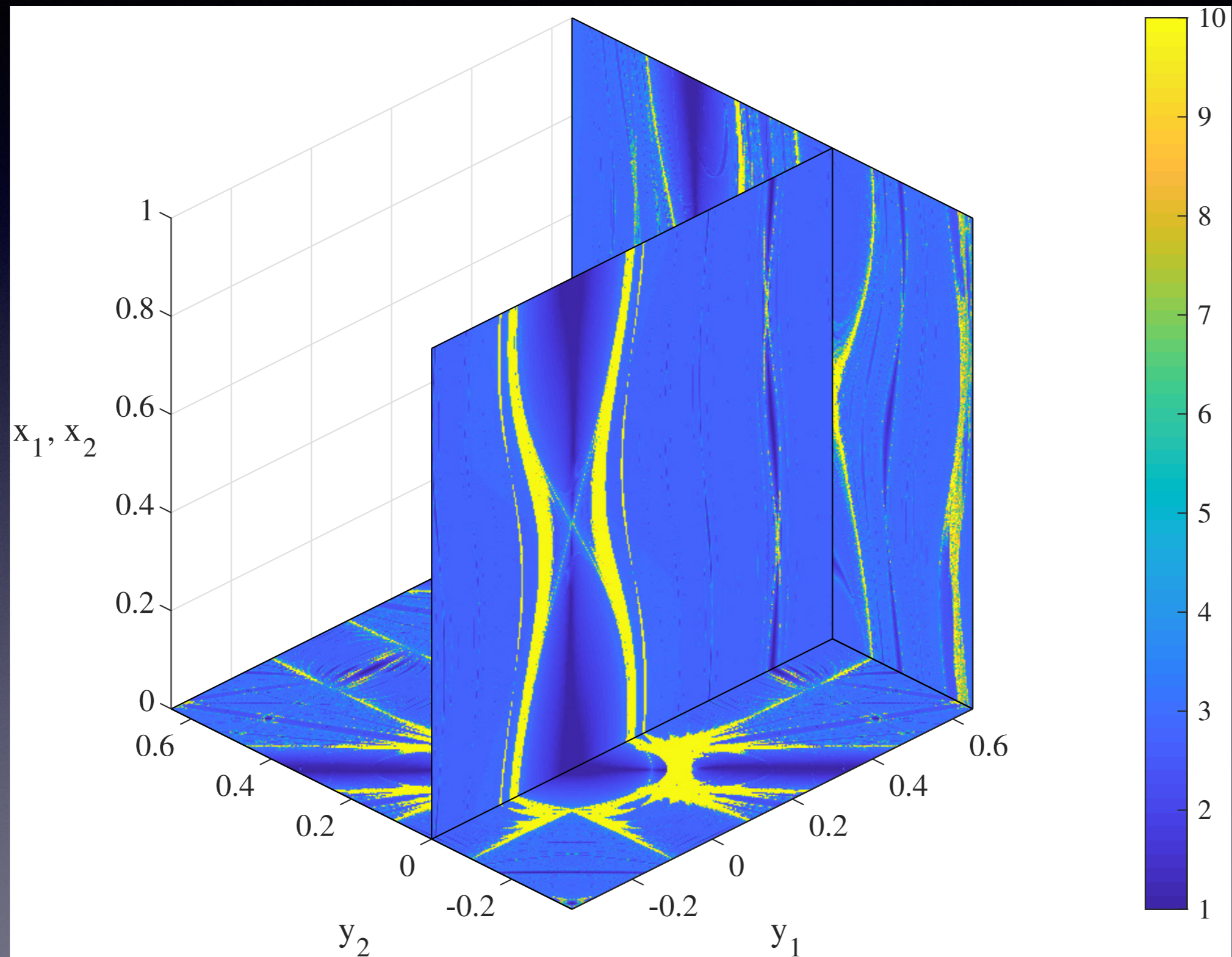
FLI, $T = 1000$

$$F = -\frac{1}{2\pi} \begin{pmatrix} a \sin(2\pi x_1) & + & c \sin(2\pi(x_1 + x_2)) \\ b \sin(2\pi x_2) & + & c \sin(2\pi(x_1 + x_2 + \varphi)) \end{pmatrix}$$

Varying Slices

($x_2=0, y_2$ varies) Slices

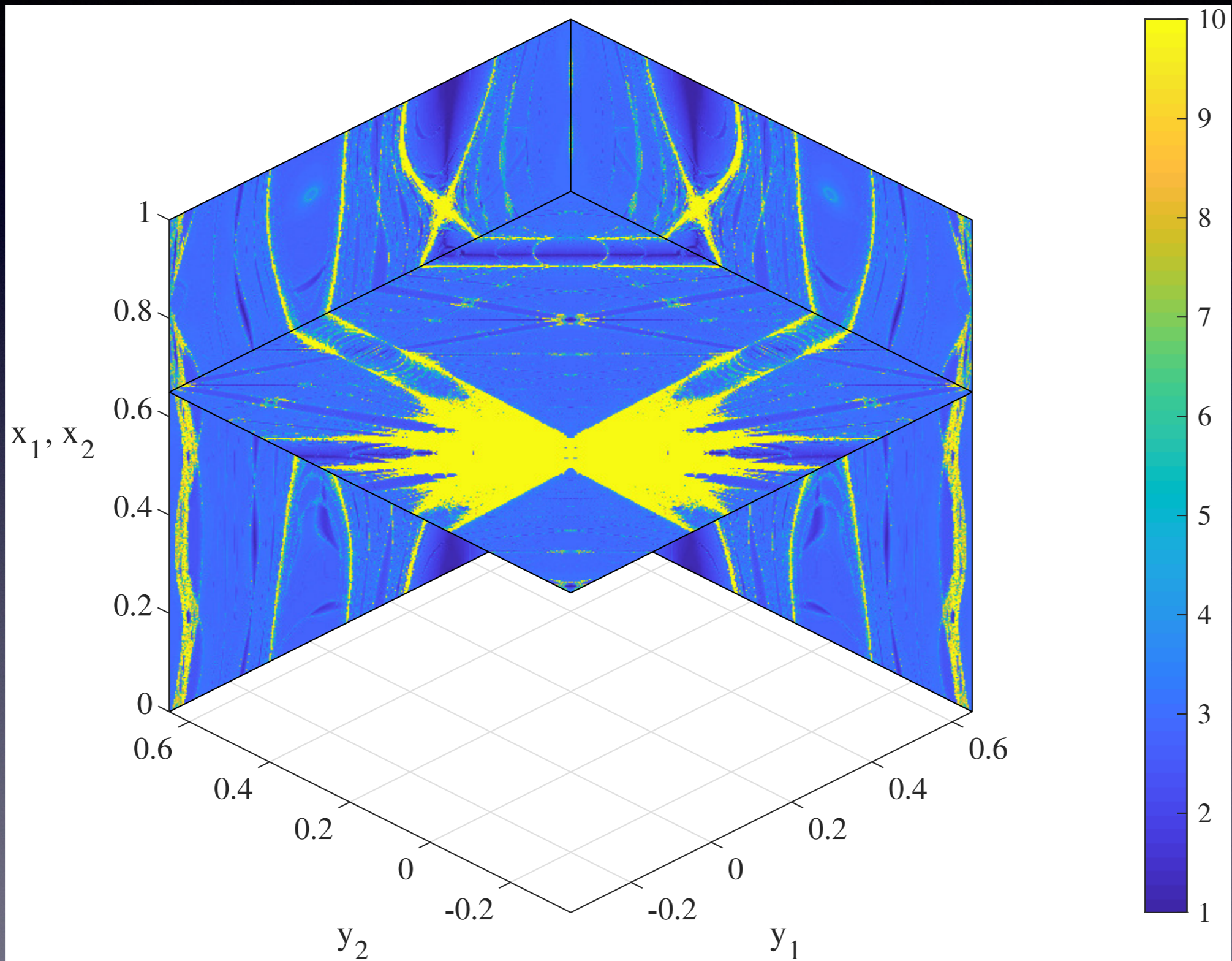
$a = 0.1$
 $b = 0.1$
 $c = 0.07$
 $\varphi = 0$



Varying Slices

$x_1 = x_2$
Slices

$a = 0.1$
 $b = 0.1$
 $c = 0.07$
 $\varphi = 0$



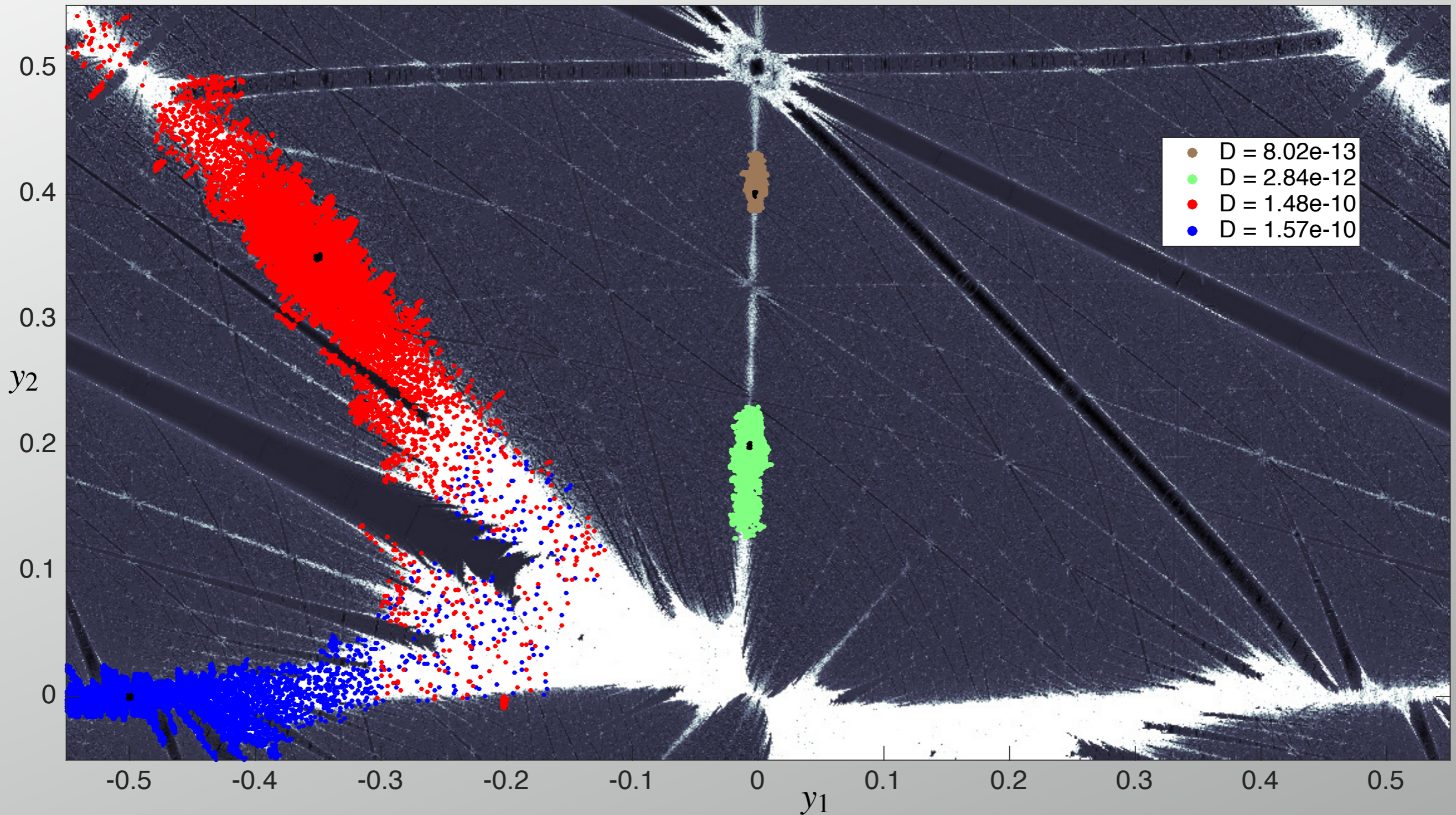
Transport

Symplectic: Diffusion

$T = 10^8$

$x = (0, 0.5)$ slice

$(a, b, c, d) = 0.0, 0.1, 0.07, 0.0001$

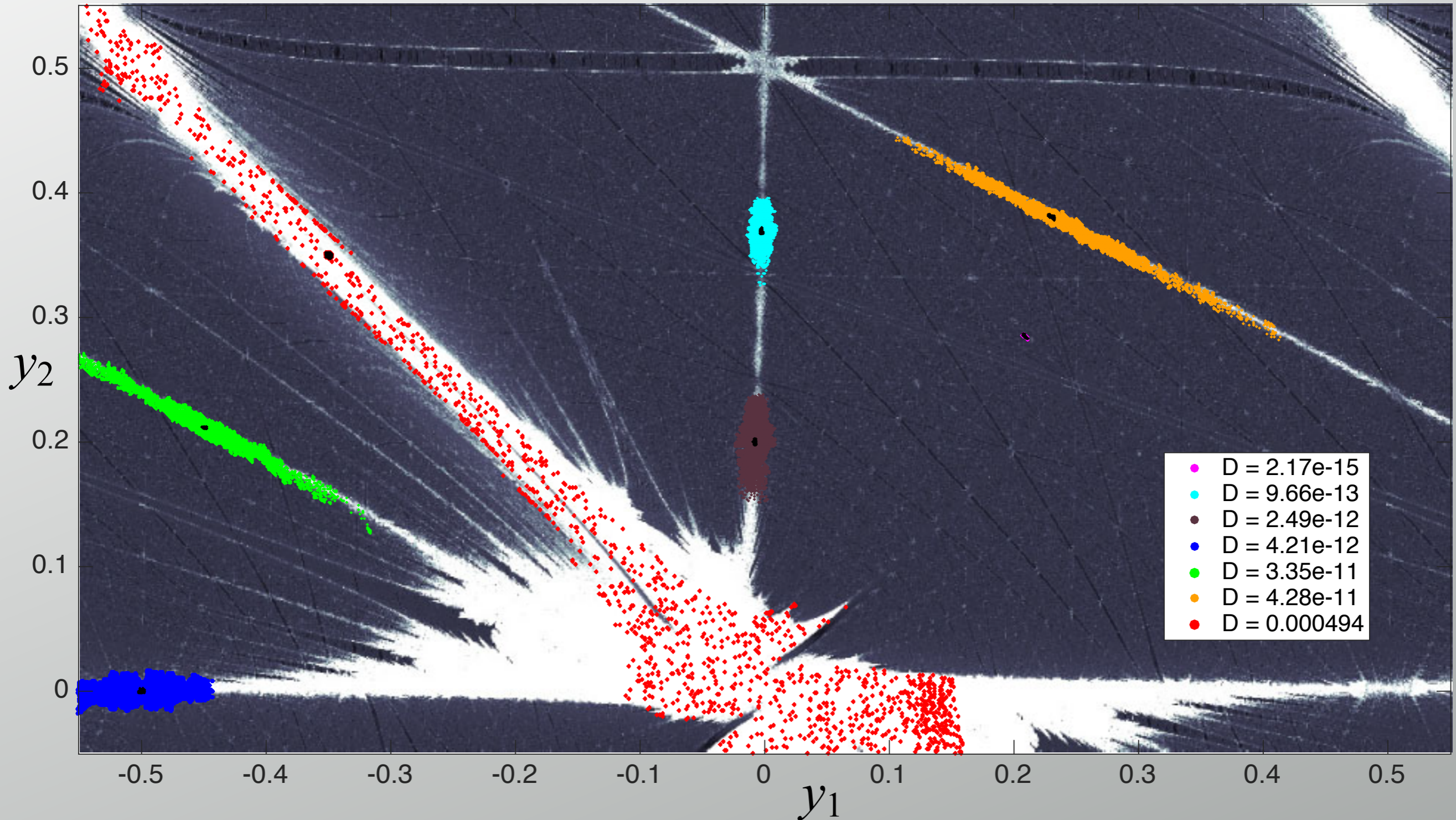


Volume Preserving: Drift

$x = (0, 0.5)$ slice

$T = 10^8$

$(a, b, c, d) = 0.0, 0.1, 0.07, 0.0001$ $\varphi = (0.5, 0)$



Structure of 4D Resonances

- Moser's Map

- 4D Quadratic Symplectic map—generalizes Hénon's map
- Local Approximation near a periodic orbit

$$M(x, y) = (x + C^{-T}(-y + Cx + \nabla U(x)), Cx)$$

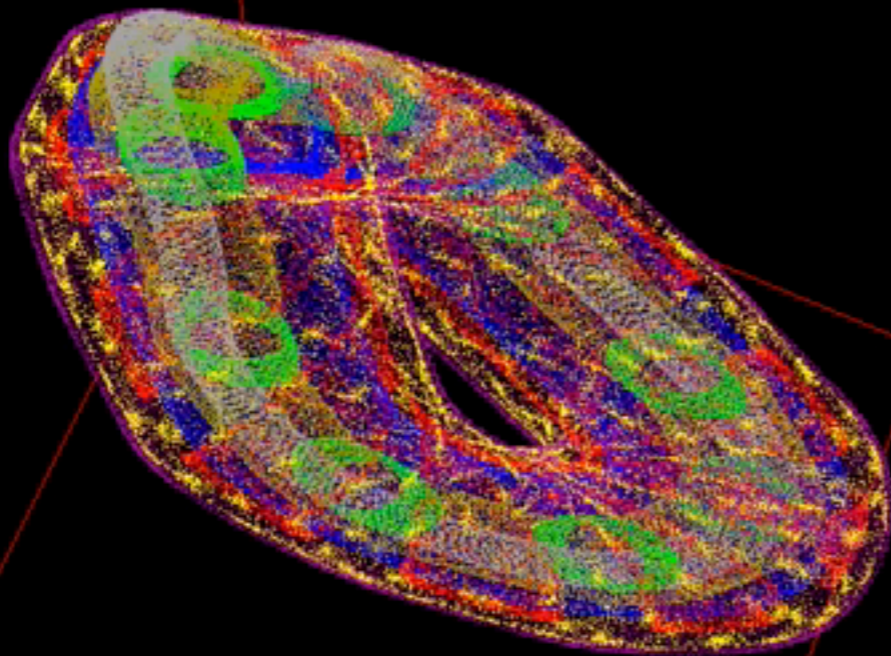
$$C = \begin{pmatrix} \alpha & \beta \\ \gamma & \delta \end{pmatrix} \quad \det(C) = \alpha\delta - \beta\gamma = \varepsilon_1 = \pm 1$$

$$U = ax_1 + bx_2 + \frac{1}{2}cx_1^2 + \varepsilon_2 x_1^3 + x_1 x_2^2 \quad \varepsilon_2 = \pm 1 \text{ or } 0$$

- 6 parameters + two discrete

3D Projection

(x_1, x_2, y_2)



$$C = \begin{pmatrix} 0 & 1 \\ 1 & 0 \end{pmatrix}$$

$$(a, b, c) = (-1.0, 0.1, 0.1)$$

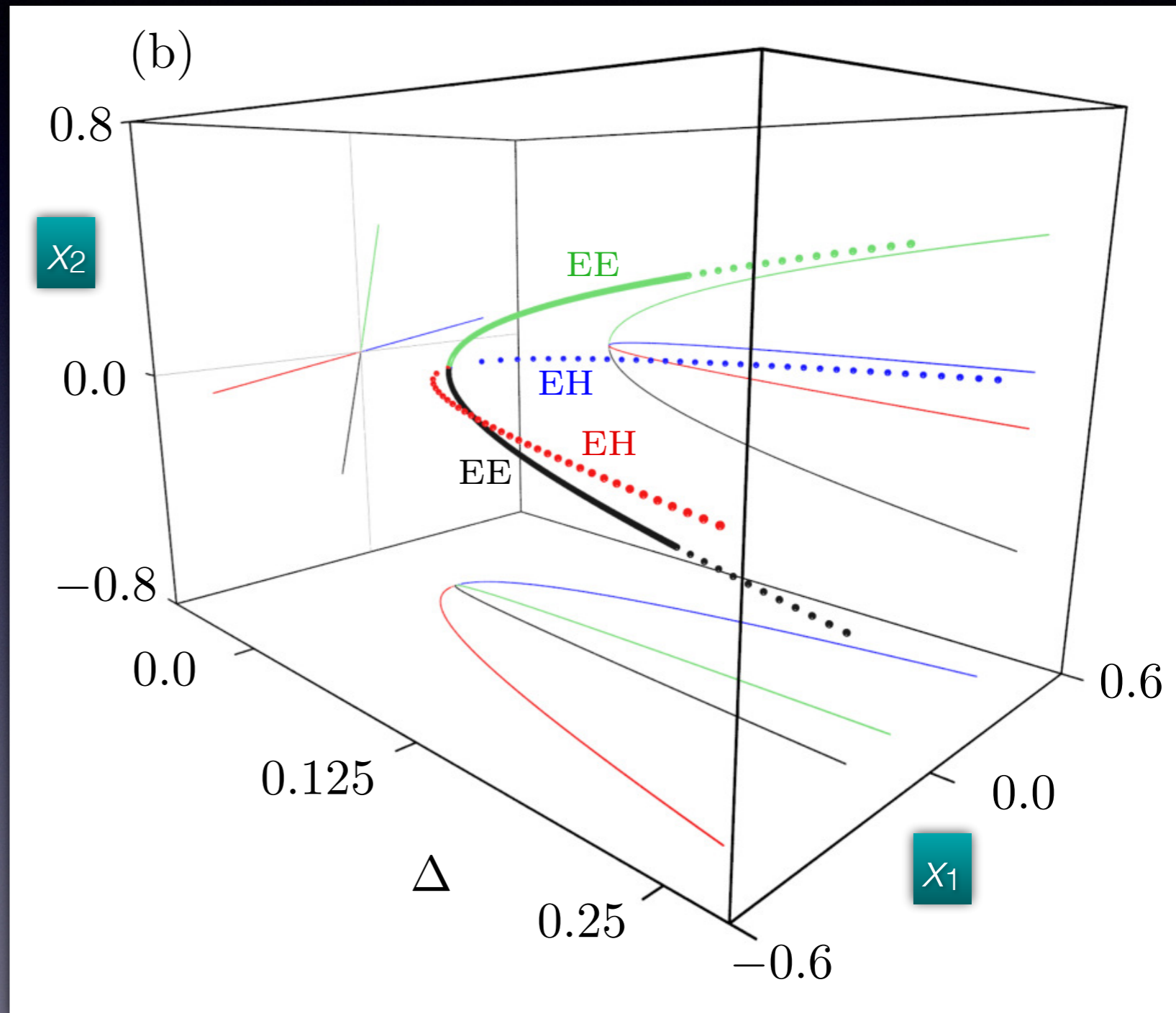
$$\varepsilon_1 = -1, \varepsilon_2 = 1$$

Fixed Points born in a Quadfurcation*

$$M(x, y) = (x + C^{-T}(-y + Cx + \nabla U(x)), Cx)$$

- When $\varepsilon_2 = 1$, a path through $a=b=c=0$ can result in a quadfurcation in a sector in parameter space.

$$(a, b, c) = -\Delta(1.5, 0.3, 1)$$



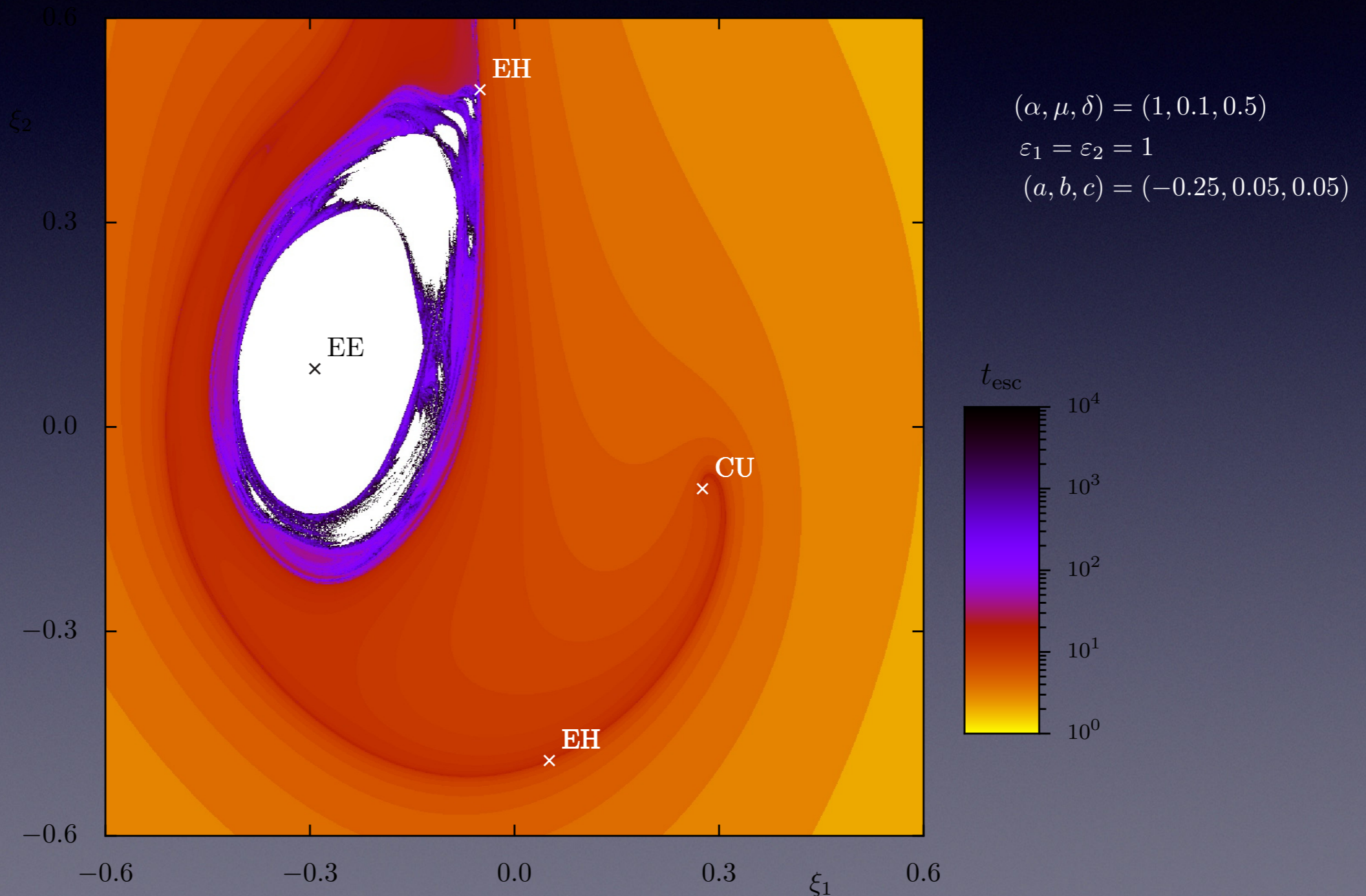
*As coined by Steve Strogatz in "Nonlinear Dynamics and Chaos"

4D Moser: Bounded Orbits

$$M(x, y) = (x + C^{-T}(-y + Cx + \nabla U(x)), Cx)$$

- Exit Time Distributions

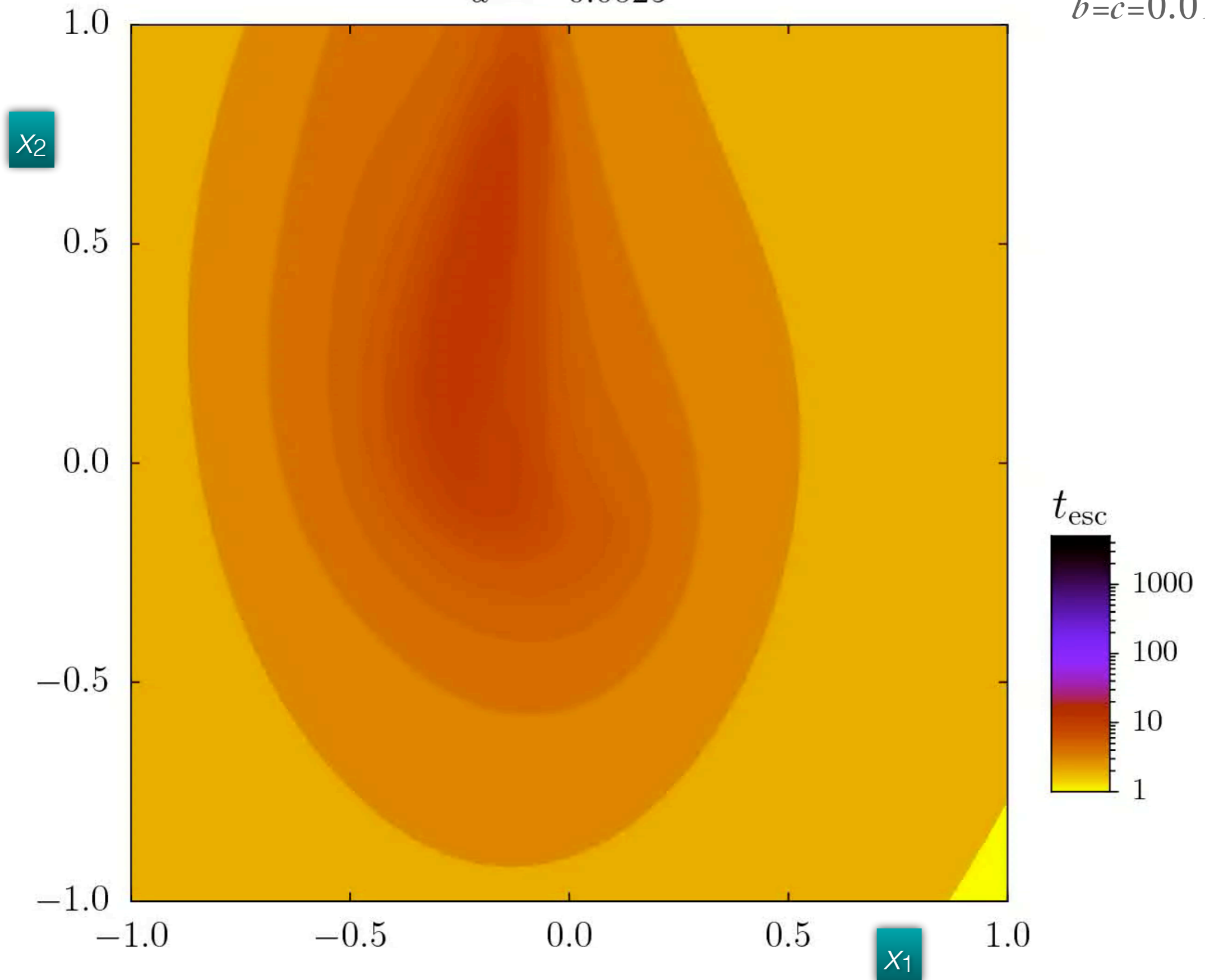
Two-plane
($x, y = Cx$)



4D Moser: Escape Time

$$a = -0.0025$$

$$b=c=0.01$$

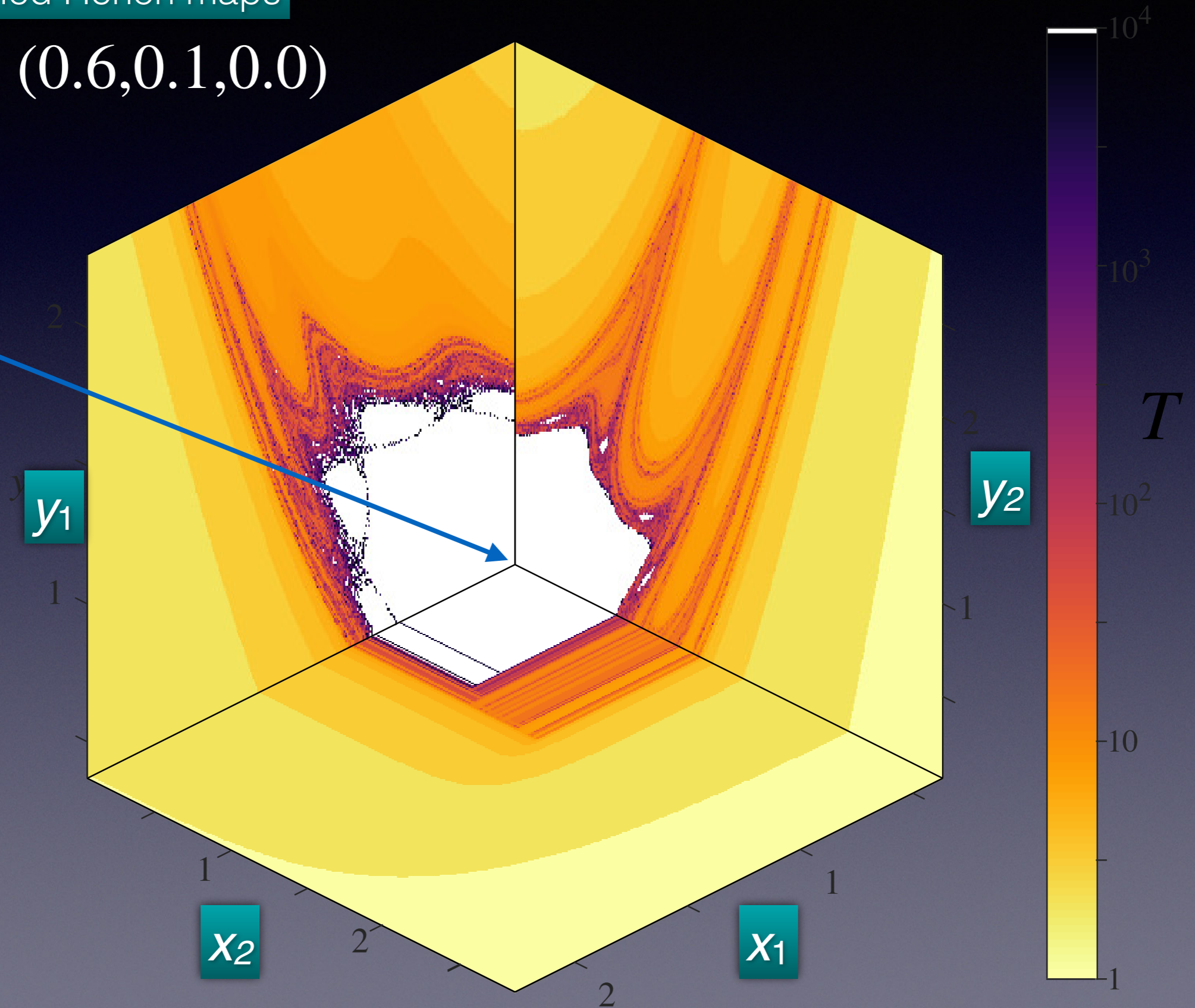


Escape Times

Pair of Uncoupled Hénon maps

$$(a_1, a_2, c) = (0.6, 0.1, 0.0)$$

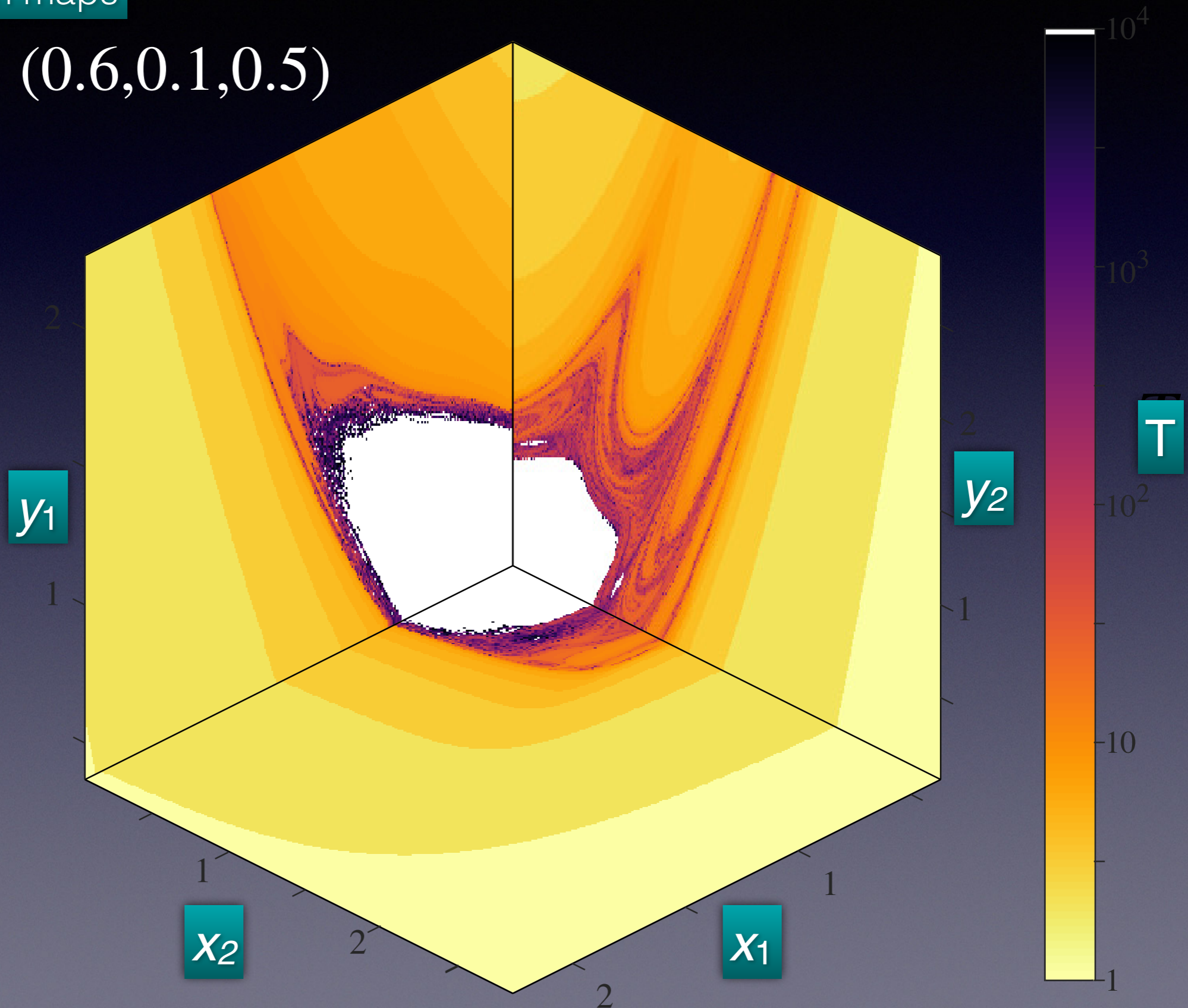
EE point



Escape Times

Coupled Hénon maps

$$(a_1, a_2, c) = (0.6, 0.1, 0.5)$$

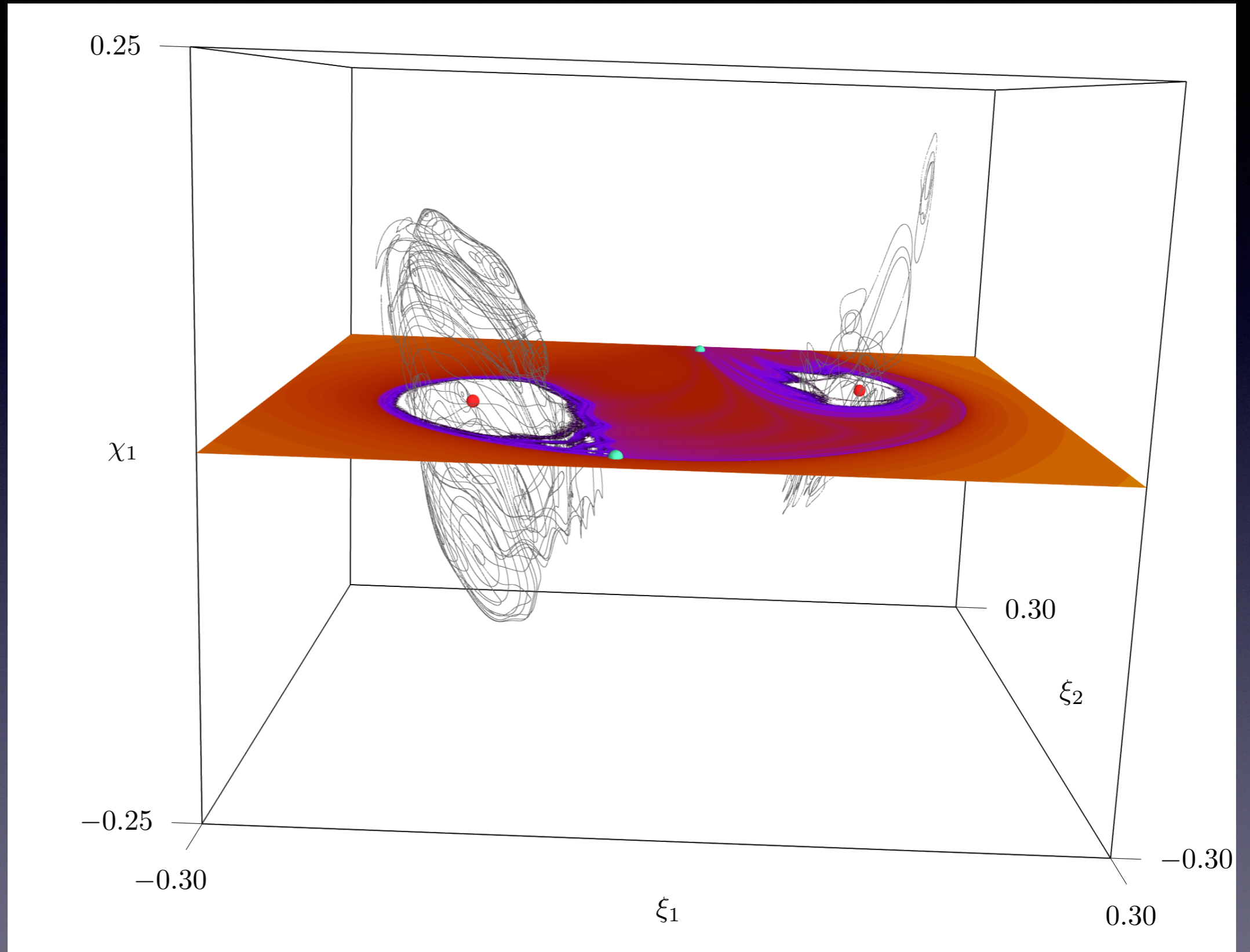


2D Escape + 3D Slices

EE + EE + EH + EH

$$\chi = C\xi$$

$$|\chi_2| < 10^{-6}$$



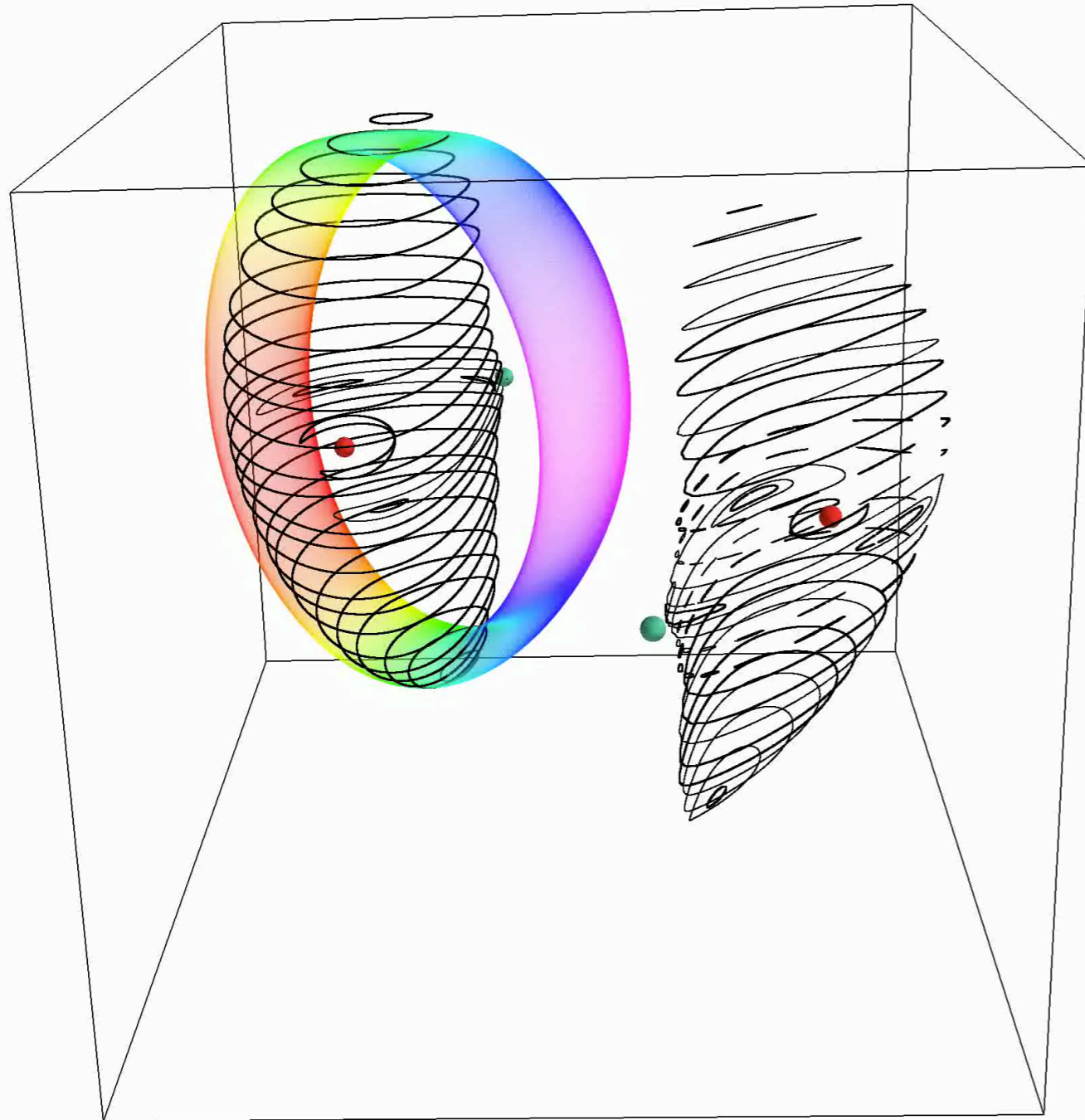
$$(a, b, c) = -0.075(1, 0.25, 0.5)$$

$$(\alpha, \beta, \mu) = (1, 1, 0.5)\varepsilon_1 = \varepsilon_2 = 1$$

Slices + Projection

- 3D Slices of Phase space ($\varepsilon_1 = 1$)

EE + EE + EH + EH



$$(a, b, c) = (-0.015, -0.005, -0.001)$$

$$(\alpha, \mu, \delta) = (1, 0.1, 0.5)$$

$$\varepsilon_1 = \varepsilon_2 = 1$$

$$(a, b, c) = (-0.0015, -0.005, -0.001)$$

Rotated coordinates
to 3-plane containing fixed
points

For More Information

- Dullin, H. R. and J. D. Meiss (2009). “Quadratic Volume-Preserving Maps: Invariant Circles and Bifurcations.” *SIAM J. Appl. Dyn. Sys.* 8(1): 76-128.
- Lomelí, H. E. and J. D. Meiss (2009). “Generating Forms for Exact Volume-Preserving Maps.” *Disc. Cont. Dyn. Sys. Series S* 2(2): 361-377.
- Dullin, H. R. and J. D. Meiss (2012). “Resonances and Twist in Volume-Preserving Mappings.” *SIAM J. Appl. Dyn. Sys.* 11: 319-349.
- Meiss, J. D. (2012). “The Destruction of Tori in Volume-Preserving Maps.” *Comm. Nonl. Sci. Num. Simul.* 17: 2108-2121.
- Fox, A. M. and J. D. Meiss (2013). “Greene's Residue Criterion for the Breakup of Invariant Tori of Volume-Preserving Maps.” *Physica D* 243(1): 45-63.
- Meiss, J. D. (2015). “Thirty years of turnstiles and transport.” *Chaos* 25(9): 097602.
- Guillery, N. and J. D. Meiss (2017). “Diffusion and Drift in Volume-Preserving Maps.” *Reg. and Chaotic Dyn.* 22(6): 700-720.
- Bäcker, A. and J. D. Meiss (2018). “Moser's Quadratic Symplectic Map.” *Reg. and Chaotic Dyn.* 23(6): 654-664.
- Meiss, J. D., N. Miguel, C. Simo and A. Vieira (2018). “Accelerator modes and anomalous diffusion in 3D volume-preserving maps.” *Nonlinearity* 31(12): 5615-5642.